

Interactions of Carbon Nanotubes with Pyrene-Functionalized Linear-Dendritic Hybrid Polymers

GREG J. BAHUN, ALEX ADRONOV

Department of Chemistry and the Brockhouse Institute for Materials Research, McMaster University, Hamilton, Ontario, Canada

Received 11 October 2009; accepted 22 November 2009

DOI: 10.1002/pola.23855

Published online in Wiley InterScience (www.interscience.wiley.com).

ABSTRACT: A series of linear-dendritic hybrid polymers, containing pyrene units at the periphery of aliphatic polyester dendrons, were prepared for the purpose of dispersing shortened single-walled carbon nanotubes (SWNTs) in tetrahydrofuran (THF). The prepared hybrids contained 1, 2, 4, 8, or 16 (G0 through G4) pyrene units and a linear segment composed of polystyrene. It was found that a minimum of four pyrene units was necessary to form a strong enough interaction with SWNTs to enable steric stabilization in solution, when using a linear polymer segment of 11.5 kDa. Increasing either the number of pyrene units per polymer chain or the length of the polymer segment to 18.0 kDa did not improve nanotube solubility, whereas decreasing the polymer length

resulted in significantly less effective nanotube dissolution. The G4 dendron alone, without the linear polystyrene segment, was also found to impart solubility to the nanotubes in THF. Interactions between the series of linear-dendritic hybrids and full-length multiwalled carbon nanotubes were also investigated, and it was found that the polymers exhibited strong interactions with the multiwalled carbon nanotube surface, resulting in the formation of stable solutions. © 2010 Wiley Periodicals, Inc. *J Polym Sci Part A: Polym Chem* 48: 1016–1028, 2010

KEYWORDS: block copolymers; dendrimers; nanocomposites; supramolecular structures; synthesis

INTRODUCTION Carbon nanotubes (CNTs) have received a great deal of attention in recent years as a result of their extraordinary mechanical strength and electronic properties.¹ These unique characteristics translate into potential applications within a variety of high-strength materials and electronic devices, including sensors, light-emitting diodes, and photovoltaics.² In many of these applications, the nanotubes are incorporated within other pre-existing materials to produce functional composites. However, for optimal performance, a uniform distribution of the CNTs within the host material is preferred and often essential.³ Given that CNTs form bundles and are inherently insoluble in aqueous and common organic solvents, they must be exfoliated into individual tubes if uniform mixing with other materials is to be achieved. It is therefore necessary to chemically functionalize CNTs with solubilizing groups, which enable exfoliation and homogenous dispersion within solvents and various host materials.

Many methods have been developed to functionalize CNTs.^{1,4–13} Much of the early work involved treatment with harsh oxidizing agents to provide carboxylic acid functionalities at the nanotube ends and defect sites, enabling further derivatization through esterification and amidation chemistry.¹ Additionally, a number of other sidewall functionalization methods, including reactions with radicals,^{1,6,14–31}

nitrenes,^{32–34} and carbenes,^{34,35} as well as dipolar cycloaddition chemistry,^{20,31,36–44} have been developed and enable attachment of various structures to the nanotube walls. However, such covalent functionalization chemistry effectively introduces defects along the nanotube walls, leading to a decrease in the strength and conductivity of the tubes.^{45,46} An alternative approach that does not cause any change to the chemical structure of the nanotubes involves supramolecular functionalization, and has received increasing recent attention.^{14,15,27,29,47–67}

Both small molecules and macromolecules have been used to disrupt nanotube bundles and provide individual nanotubes in solution, strictly by supramolecular interactions.^{68–70} The utilization of small molecules to noncovalently functionalize nanotubes has largely focused on derivatives of polycyclic aromatic hydrocarbons (PAH's), such as naphthalene, phenanthrene, and pyrene.^{69–75} Pyrene can π -stack to CNTs with a binding energy of up to 50 kJ/mol.⁷⁶ In addition to small molecules, it has also been shown that introduction of PAH's as side-chains on polymers enables supramolecular grafting of the resulting conjugates to the nanotube surface.^{77–85} Jérôme and coworkers have shown that PMMA, functionalized with pyrene units as side-chains randomly along the polymer backbone, could stabilize dispersions of multiwalled carbon nanotubes (MWNTs) in

Correspondence to: A. Adronov (E-mail: adronov@mcmaster.ca)

Journal of Polymer Science: Part A: Polymer Chemistry, Vol. 48, 1016–1028 (2010) © 2010 Wiley Periodicals, Inc.

toluene, tetrahydrofuran (THF), and chloroform.^{77,78} Increasing the concentration of pyrene on the polymers improved the solution-phase stability of the resulting materials. Our own work has investigated the role of polymer architecture and composition with linear pyrene-functionalized polystyrene polymers.⁷⁹ In our previous study, block copolymers, featuring a pyrene block, were shown to be superior in dispersing single-walled carbon nanotubes (SWNTs) when compared to polymers containing an equal amount of pyrene randomly distributed throughout the backbone. It was also shown that increasing the length of the pyrene-containing block decreased the solubility of the polymer–nanotube complexes.⁷⁹

Despite these initial encouraging results, very little has been reported about the effect of nonlinear polymer architectures on the stability of supramolecular polymer–nanotube complexes. Although branched macromolecules, such as dendrimers and hyperbranched polymers, have been used to covalently functionalize CNTs, their effectiveness in supramolecular functionalization has received comparatively little attention.⁷¹ Fewer still are the studies that have relied on π -stacking from the periphery of a dendron to increase the interactions with nanotubes in nonaqueous solvents.⁸⁶ We hypothesized that introduction of PAH's, such as pyrene, at the periphery of a dendrimer would not only provide a compact, globular architecture that may preorganize the peripheral pyrene groups around the nanotube, but would also produce structures in which the number of binding groups available in each macromolecule is precisely known. Here, we report the preparation of pyrene-functionalized linear-dendritic polymer hybrids and their ability to form non-covalent complexes with SWNTs that are soluble in organic solvents.

EXPERIMENTAL

Materials

SWNTs were purchased from Carbon Nanotechnologies (Houston, TX) and shortened according to previously published procedures.²³ MWNTs (purchased from Nanocyl, Belgium, Nanocyl-7000, 90% purity, Lot 257-1) were used as received. Benzylidene anhydride (**2**) was synthesized according to literature procedures.⁸⁷ Compounds **3–10** were synthesized according to previously published procedures.⁸⁸ All other reagents were obtained from Acros or Aldrich and used without further purification. Column chromatography was carried out with Silica Gel 60 (230–400 mesh, ASTM).

Techniques

NMR spectra were measured on Bruker DRX 500 MHz and Avance 600 MHz spectrometers. ¹H spectra were recorded at 500 or 600 MHz and ¹³C NMR spectra were recorded at 125 or 150 MHz in CDCl₃. The nondeuterated solvent signal was used as the internal standard for both ¹H and ¹³C spectra. MALDI-TOF mass spectrometry was performed using a Micromass TofSpec 2E spectrometer in positive ion mode using 2-(4-hydroxyphenyl-azo) benzoic acid (HABA) as the matrix. Polymer molecular weight and polydispersity index (PDI) were estimated by size exclusion chromatography

(SEC) using a Waters 2695 separations module equipped with a Waters 2414 refractive index detector and three Polymer Labs PLgel individual pore size columns, with 5 μ m bead size and pore sizes of 100, 10³, and 10⁵ Å, at a constant temperature of 40 °C. Polystyrene standards were used for calibration, and THF was used as the mobile phase at a flow rate of 1.0 mL/min. Raman spectroscopy was performed on a Renishaw InVia Raman spectrometer equipped with a 25 mW argon ion laser (514 nm), a 300 mW Renishaw 785 nm laser, 1800 l/mm and 1200 l/mm gratings for the two lasers, respectively, and a high-resolution mapping stage. The Raman system is also equipped with a Leica microscope having 5 \times , 20 \times , and 50 \times objectives as well as a USB camera for sample viewing. UV-Vis spectroscopy was performed using a Varian Cary 50 spectrophotometer. Fluorescence spectra were measured using a Jobin-Yvon SPEX Fluorolog 3.22 equipped with a 450 W Xe lamp, double-excitation and double-emission monochromators, and a digital photon-counting photomultiplier. Slit widths were set to 0.9 nm bandpass on both excitation and emission. Correction for variations in lamp intensity over time and λ was achieved using a reference silicon photodiode.

Synthesis of TSe-G1-Py₂ (**11a**) (General Procedure for Coupling Pyrene Butyric Acid to Peripheral Alcohols)

TSe-G1-OH₂ (**4**) (0.148 g, 0.468 mmol, 1 equiv) was added to a flame-dried flask equipped with a magnetic stir bar along with pyrene butyric acid (0.394 g, 1.3 mmol, 2.9 equiv), EDC (0.263 g, 1.4 mmol, 2.9 equiv), and DMAP (0.026 g, 0.2 mmol, 0.8 equiv). Dry DCM was added (4 mL) and the mixture was stirred overnight. The solvent was evaporated in vacuo, and column chromatography on silica gel was used to purify the product (eluent: 100% DCM, then 98:2 DCM:EtOAc). Yield: 0.32 g (80%).

¹H NMR (600 MHz, CDCl₃): δ = 1.14 (s, 3 H), 2.14 (quintet, J = 7.4 Hz, 4 H), 2.32 (s, 3 H), 2.43 (t, J = 7.2 Hz, 4 H), 3.33 (m, 6 H), 4.17 (m, 4 H), 4.40 (t, J = 6 Hz, 2 H), 7.22 (d, J = 7.9 Hz, 2 H), 7.70 (d, J = 8.1 Hz, 2 H), 7.79–8.25 (m, 18 H). ¹³C NMR (150 MHz, CDCl₃): δ = 17.7, 21.6, 26.7, 32.8, 33.7, 46.4, 55.0, 58.3, 65.2, 123.3, 124.9, 125.0, 125.2, 126.0, 126.8, 127.4, 127.6, 128.1, 128.8, 130.1, 131.0, 131.5, 135.6, 136.2, 145.2, 172.4, and 173.0. MS Calc'd for C₅₄H₄₈O₈S [M]⁺ m/z = 856.31, [M + NH₄]⁺ m/z = 874.34. Found ES MS: [M + NH₄]⁺ = 874.4, high-resolution ES MS: [M + NH₄]⁺ = 874.3447.

Synthesis of HOOC-G1-Py₂ (**11b**) (General Procedure Removal of TSe Group)

The TSe-G1-Py₂ (**11a**) (0.428 g, 0.5 mmol, 1 equiv) was added to a round-bottom flask equipped with a stir bar. This was dissolved in toluene (5 mL), before adding DBU to the mixture (0.38 g, 2.5 mmol, 5 equiv). The reaction was monitored by TLC (EtOAc:hexanes 2:1). Upon consumption of starting material (R_f = 0.75), ethyl acetate (10 mL) was added and the solution was washed with 20% NaHSO₄ (3 \times 25 mL). The organic layer was concentrated down, and precipitated from an ethyl acetate solution into hexanes. The solid was filtered and dried to give 0.30 g of product (88%).

^1H NMR (200 MHz, d_6 -DMSO): δ = 1.14 (s, 3 H), 1.96 (m, 4 H), 2.43 (t, J = 7.1 Hz, 4 H), 3.25 (t, J = 7.5 Hz, 4 H), 4.21 (m, 4 H), and 7.77–8.35 (m, 18 H). ^{13}C NMR (125 MHz, d_6 -DMSO): δ = 18.0, 27.1, 32.3, 33.6, 45.9, 65.6, 123.8, 124.6, 124.7, 125.2, 125.3, 126.5, 127.0, 127.7, 127.8, 128.6, 129.8, 130.8, 131.3, 136.5, 172.9, and 174.6. MS Calc'd for $\text{C}_{45}\text{H}_{38}\text{O}_6$ $[\text{M}]^+$ m/z = 674.78, $[\text{M} + \text{NH}_4]^+$ m/z = 692.30. Found ES MS: $[\text{M} + \text{NH}_4]^+$ = 692.2, high-resolution ES MS: $[\text{M} + \text{NH}_4]^+$ = 692.3000.

Synthesis of TSe-G2-Py₄ (12a)

The general procedure for coupling pyrene butyric acid to peripheral alcohols was followed. TSe-G2-OH₄ (**6**) (0.148 g, 0.27 mmol, 1 equiv) pyrene butyric acid (0.394 g, 1.3 mmol, 5 equiv), EDC (0.263 g, 1.4 mmol, 5.1 equiv), and DMAP (0.026 g, 0.2 mmol, 0.8 equiv) were added to a flame-dried flask equipped with a magnetic stir bar. Dry DCM was added (4 mL) and the mixture was stirred overnight. The solvent was removed, and column chromatography on silica gel was used to purify the product (100% DCM, then 98:2 DCM:EtOAc). Yield: 0.27 g (62%).

^1H NMR (500 MHz, CDCl_3): δ = 1.04 (s, 3 H), 1.18 (s, 6H), 2.11 (q, J = 7.5 Hz, 8 H), 2.23 (s, 3 H), 2.41 (t, J = 7.2 Hz, 8 H), 3.25–3.31 (m, 10 H), 4.11 (broad s, 4 H), 4.21 (m, 8 H), 4.33 (t, J = 5.8 Hz, 2 H), 7.14 (d, J = 8.1 Hz, 2 H), 7.65 (d, J = 8.2 Hz, 2 H), and 7.74–8.28 (m, 36 H). ^{13}C NMR (150 MHz, CDCl_3): δ = 14.3, 17.3, 17.9, 21.5, 26.7, 32.7, 33.6, 46.5, 54.8, 58.3, 60.5, 65.3, 65.5, 77.2, 123.3, 124.9, 124.9, 125.0, 125.1, 125.9, 126.8, 127.3, 127.5, 127.5, 128.0, 128.8, 130.0, 130.9, 131.5, 135.6, 172.1, and 173.0. MS Calc'd for $\text{C}_{104}\text{H}_{92}\text{O}_{16}\text{S}$ $[\text{M}]^+$ m/z = 1629.90. Found MALDI-TOF MS: $[\text{M} + \text{Na}]^+$ m/z = 1629.

Synthesis of HOOC-G2-Py₄ (12b)

The general procedure for TSe removal was followed. TSe-G2-Py₄ (**12a**) (0.160 g, 0.1 mmol, 1 equiv) was combined with DBU (0.030 g, 0.2 mmol, 2 equiv) in a round-bottom flask equipped with a magnetic stir bar. Toluene was added (1.5 mL) and the reaction was stirred at room temperature for 1 h. Upon consumption of starting material (R_f = 0.75), ethyl acetate (10 mL) was added and the solution was washed with 20% NaHSO_4 (3 \times 25 mL). The organic layer was concentrated down, and precipitated from an ethyl acetate solution into hexanes. Yield: 0.12 g (87%).

^1H NMR (600 MHz, CDCl_3): δ = 1.14 (s, 3 H), 1.18 (s, 6 H), 2.08 (quintet, J = 7.7 Hz, 8 H), 2.39 (t, J = 7.2 Hz, 8 H), 3.24 (t, J = 7.7 Hz, 8 H), 4.18–4.26 (m, 12 H), 7.70–8.18 (m, 36 H). ^{13}C NMR (150 MHz, CDCl_3): δ = 17.5, 17.9, 26.7, 32.7, 33.6, 46.4, 46.5, 65.4, 65.7, 123.3, 124.9, 125.0, 125.1, 125.4, 125.9, 126.8, 127.3, 127.5, 127.8, 128.1, 128.7, 130.0, 130.9, 131.4, 135.5, 172.1, 173.1, and 175.5. MS Calc'd for $\text{C}_{95}\text{H}_{82}\text{O}_{14}$ $[\text{M}]^+$ m/z = 1447.66, $[\text{M} + \text{Na}]^+$ = 1469.56. Found MALDI-TOF MS: $[\text{M} + \text{Na}]^+$ m/z = 1472.

Synthesis of TSe-G3-Py₈ (13a)

The general procedure for coupling pyrene butyric acid to peripheral alcohols was followed. TSe-G3-OH₈ (**8**) (0.614 g, 0.6 mmol, 1 equiv), pyrene butyric acid (3.043 g, 10.6 mmol,

17 equiv), EDC (2.224 g, 11.6 mmol, 19.2 equiv), and DMAP (0.052 g, 0.17 mmol, 0.3 equiv) were added to a flame-dried flask equipped with a magnetic stir bar. Dry DCM was added (10 mL) and the mixture was stirred overnight. The solvent was evaporated in vacuo, and the product was purified by column chromatography on silica gel (5:0.6:0.4, DCM:hexanes:EtOAc). Yield: 1.55 g (82%).

^1H NMR (500 MHz, CDCl_3): δ = 1.15 (s, 3 H), 1.17 (s, 6 H), 1.19 (s, 12 H), 2.08 (quintet, J = 7.5 Hz, 16 H), 2.18 (s, 3 H), 2.40 (t, J = 7.2 Hz, 16 H), 3.24 (t, J = 7.8 Hz, 18 H), 4.1–4.3 (m, 28 H), 4.34 (t, J = 6.2 Hz, 2 H), 7.05 (d, J = 8.7 Hz, 2 H), 7.60 (d, J = 8.5 Hz, 2 H), 7.65–8.20 (m, 72 H). ^{13}C NMR (150 MHz, CDCl_3): δ = 17.3, 17.6, 17.9, 21.5, 26.7, 32.7, 33.6, 46.6, 46.6, 46.8, 54.7, 58.3, 65.3, 65.4, 66.2, 123.3, 124.8, 124.9, 124.9, 125.0, 125.1, 125.9, 126.7, 127.3, 127.4, 127.5, 127.9, 128.7, 130.0, 130.9, 131.5, 135.6, 136.4, 145.0, 171.2, 171.6, 172.2, and 173.0. MS Calc'd for $\text{C}_{204}\text{H}_{180}\text{O}_{32}\text{S}$ $[\text{M}]^+$ m/z = 3173.2, $[\text{M} + \text{Na}]^+$ m/z = 3196.2. Found MALDI-TOF MS: $[\text{M} + \text{Na}]^+$ m/z = 3198.7.

Synthesis of HOOC-G3-Py₈ (13b)

The general procedure for TSe removal was followed. TSe-G3-Py₈ (**13a**) (0.160 g, 0.1 mmol, 1 equiv) was combined with DBU (0.030 g, 0.2 mmol, 2 equiv) in a round-bottom flask equipped with a magnetic stir bar. Toluene was added (1.5 mL) and the reaction was stirred at room temperature. Upon consumption of starting material, CH_2Cl_2 (10 mL) was added and the solution was washed with 20% NaHSO_4 (3 \times 25 mL). The organic layer was concentrated down, and precipitated from an ethyl acetate solution into hexanes. Yield: 0.124 g (82%).

^1H NMR (600 MHz, CDCl_3): δ = 1.09 (s, 6 H), 1.14 (s, 12 H), 1.22 (s, 3 H), 2.05 (quintet, J = 7.3 Hz, 16 H), 2.36 (broad m, 16 H), 3.21 (t, J = 7.7 Hz, 16 H), 4.1–4.3 (m, 28 H), 7.6–8.2 (m, 72 H). ^{13}C NMR (150 MHz, CDCl_3): δ = 17.4, 17.6, 17.9, 26.7, 31.0, 32.5, 32.7, 33.6, 46.5, 46.8, 65.2, 65.4, 68.5, 123.3, 124.8, 124.9, 125.0, 125.0, 125.1, 125.9, 126.7, 127.3, 127.5, 127.5, 128.7, 130.0, 130.9, 131.4, 135.6, 172.2, 172.2, 172.4, and 173.0. MS Calc'd for $\text{C}_{195}\text{H}_{170}\text{O}_{30}$ $[\text{M}]^+$ m/z = 2991.2, $[\text{M} + \text{Na}]^+$ m/z = 3014.2. Found MALDI-TOF MS: $[\text{M} + \text{Na}]^+$ m/z = 3017.9.

Synthesis of TSe-G4-Py₁₆ (14a)

The general procedure for coupling pyrene butyric acid to peripheral alcohols was followed. 1-Pyrenebutyric acid (0.249 g, 0.86 mmol, 24 equiv), EDC, (0.172 g, 0.9 mmol, 25 equiv), DPTS (0.001 g, 3.6×10^{-6} mol, 0.1 equiv) and TSe-G4-OH₁₆ (**10**) (0.070 g, 3.6×10^{-5} mol) were added to 0.7 mL of dichloromethane in a round-bottom flask equipped with a magnetic stir bar. The mixture was stirred for 3 days after which MALDI indicated the reaction had not reached complete conversion. Additional pyrene butyric acid (0.125 g, 0.4 mmol, 12 equiv) and EDC (0.090 g, 0.47 mmol, 13 equiv) were added and the reaction was stirred for further 2 days. At this time, the MALDI showed only the final product. The product was purified using column chromatography (4.0:0.5:0.5 DCM:hexanes:EtOAc as the eluent) and dried

overnight in vacuo to yield 0.165 g (75%) of a white powder.

^1H NMR (500 MHz, CDCl_3): δ = 1.15 (broad m, 45H), 1.99 (quintet, J = 6.8 Hz, 32 H), 2.31 (t, J = 7.1 Hz, 35 H), 3.13 (t, J = 7.7 Hz, 34 H), 4.09–4.28 (broad m, 60 H), 4.31 (t, J = 5.4 Hz, 2 H), 6.88 (d, J = 8 Hz, 2 H), 7.48 (d, J = 8 Hz, 2 H), and 7.55–8.08 (m, 144 H). ^{13}C NMR (125 MHz, CDCl_3): δ = 17.2, 17.5, 17.6, 17.9, 26.6, 32.6, 33.6, 46.5, 46.7, 65.1, 65.2, 65.7, 66.6, 123.2, 124.8, 124.9, 125.0, 125.8, 126.7, 127.2, 127.4, 127.4, 127.8, 128.6, 129.9, 130.8, 131.4, 135.5, 171.5, 171.6, 171.7, 172.1, and 172.9. MS Calc'd for $\text{C}_{404}\text{H}_{356}\text{O}_{64}\text{S}$ $[\text{M}]^+$ m/z = 6262.4, $[\text{M} + \text{K}]^+$ m/z = 6301.4. Found MALDI-TOF MS: $[\text{M} + \text{K}]^+$ m/z = 6318.0.

Synthesis of HOOC-G4-Py₁₆ (14b)

The general procedure for TSe removal was followed. The TSe-G4-Py₁₆ (14a) (0.165 g, 2.6×10^{-5} mol, 1 equiv) was dissolved in toluene (0.4 mL) and upon addition of DBU (0.022 g, 0.1 mmol, 5 equiv) was stirred at room temperature. The mixture was stirred overnight, after which no starting material could be observed by TLC. The mixture was diluted with 5 mL of CH_2Cl_2 , and then washed with 20% NaHSO_4 (3×10 mL) followed by brine (1×10 mL) before being dried with Na_2SO_4 . Filtering off the drying agent followed by precipitation into hexanes yielded 0.145 g of the acid (91%).

^1H NMR (500 MHz, CDCl_3): δ = 1.12 (broad s, 42H), 1.20 (s, 3 H), 2.01 (quintet, J = 7.5 Hz, 32 H), 2.32 (t, J = 7.1 Hz, 32 H), 3.15 (t, J = 7.8 Hz, 32 H), 4.10–4.28 (broad m, 60 H), and 7.55–8.10 (m, 144 H). ^{13}C NMR (125 MHz, CDCl_3): δ = 17.4, 17.5, 17.8, 26.5, 32.5, 33.5, 46.4, 46.7, 65.1, 65.3, 123.1, 124.7, 124.8, 124.9, 125.0, 125.7, 126.6, 127.1, 127.3, 127.4, 128.6, 129.9, 130.8, 131.3, 135.4, 171.4, 172.1, 172.2, and 172.9. MS Calc'd for $\text{C}_{395}\text{H}_{346}\text{O}_{62}$ $[\text{M}]^+$ m/z = 6080.4, $[\text{M} + \text{K}]^+$ m/z = 6119.4. Found MALDI-TOF MS: $[\text{M} + \text{K}]^+$ m/z = 6139.1.

Synthesis of PS-G0-Py (15)

11.5 kDa Polystyrene (0.200 g, 0.017 mmol, 1 equiv) was added to a round-bottom flask with KI (2 mg, 0.012 mmol, 0.7 equiv) and K_2CO_3 (2.7 mg, 0.02 mmol, 1.1 equiv). This was dissolved in 0.5 mL of DMF and stirred for 30 min. Finally, pyrene butyric acid was added (18 mg, 0.06 mmol, 3.6 equiv) and the mixture was stirred at 90 °C. After 2 days, the contents were extracted into DCM, and washed with water (2×20) and 20% NaHSO_4 (aq) (3×10). The organic layer was dried and the product was purified by column chromatography (100% DCM) to yield 0.185 g (90%). SEC: M_w = 12,050 g/mol, M_w/M_n = 1.09.

^1H NMR (600 MHz, CDCl_3): δ = 1.25–2.29 (broad m), 2.50 (broad, 2H), 3.34–3.43 (broad m, 2 H), 5.00–5.13 (broad m, 2 H), 6.28–7.25 (broad m), and 7.80–8.30 (m, 9 H). ^{13}C NMR (150 MHz, CDCl_3): δ = 11.6, 14.3, 14.5, 18.9, 19.6, 20.6, 20.9, 22.8, 25.4, 27.0, 27.8, 28.4, 29.2, 29.8, 31.7, 32.9, 34.0, 34.7, 34.8, 36.2, 40.5–40.8, 42.7, 43.6, 44.0, 44.3, 46.0–46.6, 66.6, 123.5–128.7, 130.1, 131.0, 131.6, 135.8, 145.2–146.2, and 173.4.

Synthesis of PS-G1-Py₂ (11c)

11.5 kDa Polystyrene (0.200 g, 0.017 mmol, 1 equiv) was added to a round-bottom flask with KI (2 mg, 0.012 mmol, 0.7 equiv) and K_2CO_3 (2.7 mg, 0.02 mmol, 1.1 equiv). This was dissolved in 0.5 mL of DMF, followed by addition of the G1 acid (11b) (0.042 g, 0.06 mmol, 3.6 equiv), and the reaction mixture was stirred at 40 °C. The reaction was monitored by TLC (3:1 DCM:hexanes) and after 2 days, the mixture was diluted in DCM (5 mL), washed with 20% NaHSO_4 (4×10 mL), and dried. The product was purified by column chromatography (3:1 DCM:hexanes, 100% DCM) and precipitated into hexanes to give 0.174 g of white solid (82%). SEC: M_w = 12,100 g/mol, M_w/M_n = 1.07.

^1H NMR (500 MHz, CDCl_3): δ = 1.22–2.30 (broad m), 2.34–2.44 (broad m, 4 H), 3.31 (broad, 4 H), 4.25–4.39 (broad m, 4 H), 5.00–5.13 (broad m, 2 H), 6.30–7.25 (broad m), 7.76–8.26 (m, 18 H). ^{13}C NMR (125 MHz, CDCl_3): δ = 11.6, 14.2, 18.9, 20.9, 22.8, 25.5, 29.2, 31.7, 32.8, 34.7, 34.8, 40.6, 40.9, 44.1, 44.4, 65.6, 124.9–128.9, 145.3, 145.4, 145.5, 145.6, 145.8, and 146.0.

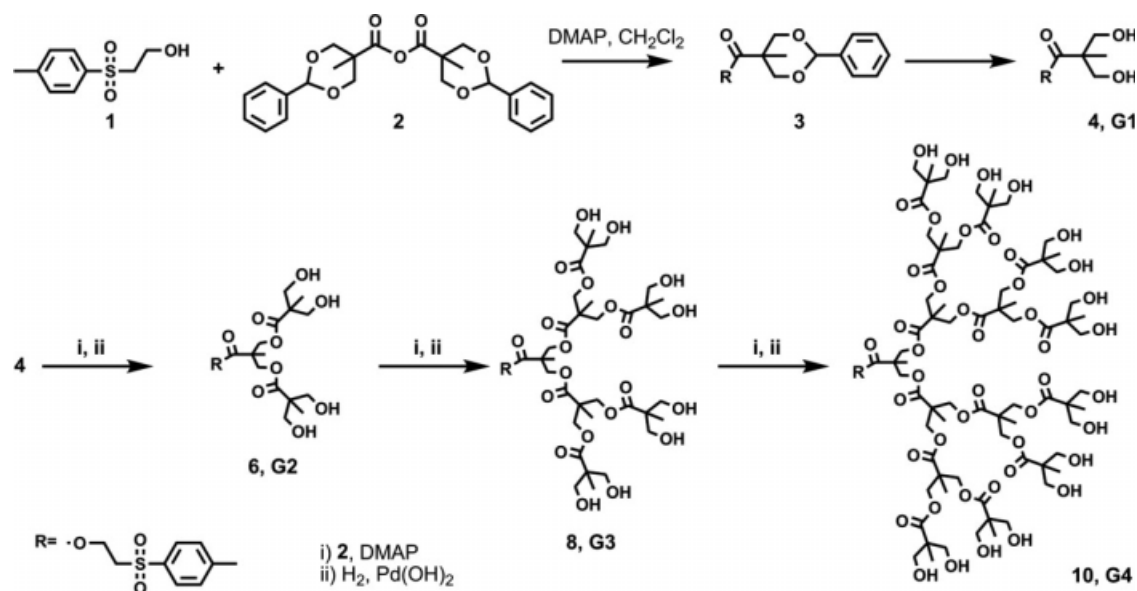
Synthesis of PS-G2-Py₄ (12c)

11.5 kDa Polystyrene (0.200 g, 0.017 mmol, 1 equiv) was added to a round-bottom flask with KI (2 mg, 0.012 mmol, 0.7 equiv) and K_2CO_3 (2.7 mg, 0.02 mmol, 1.1 equiv). This was dissolved in 0.5 mL of DMF, followed by addition of the G2 acid (12b) (0.145 g, 0.1 mmol, 5.8 equiv), and the reaction mixture was stirred at 40 °C. The reaction was monitored by TLC (3:1 DCM:hexanes). After 3 days, the mixture was diluted in DCM (5 mL), washed with 20% NaHSO_4 (4×10 mL), and dried. The product was separated by column chromatography (3:1 DCM:hexanes, 100% DCM), and precipitated into hexanes to yield 0.163 g of white powder. Yield: 0.163 g (72%). SEC: M_w = 13,000 g/mol, M_w/M_n = 1.06.

^1H NMR (600 MHz, CDCl_3): δ = 1.35–2.35, 2.36–2.41 (t, J = 7.2 Hz, 8 H), 3.23–3.29 (t, J = 7.6 Hz, 8 H), 4.14–4.25 (m, 12 H), 4.93–5.03 (broad m, 2 H), 6.28–7.25 (broad m), and 7.5–8.3 (m, 36 H). ^{13}C NMR (150 MHz, CDCl_3): δ = 11.6, 14.3, 17.7, 17.9, 18.9, 20.9, 21.3, 22.4, 22.8, 22.8, 25.4, 26.7, 28.4, 28.6, 29.2, 29.5, 29.8, 31.7, 32.1, 32.7, 33.6, 33.9, 34.7, 34.8, 36.2, 40.4–40.8, 41.9, 42.5–42.9, 43.6, 44.0, 44.3, 45.0, 45.1, 45.6–46.3, 46.5, 46.6, 46.7, 65.3, 65.7, 123.3, 124.9, 124.9, 125.0, 125.1, 125.2, 125.6, 125.8, 125.9, 126.8, 127.3–128.4, 128.8, 130.1, 131.0, 131.5, 135.6, 145.0–146.2, 172.0, 172.2, and 173.0.

Synthesis of PS-G3-Py₈ (13c)

11.5 kDa Polystyrene (0.300 g, 0.026 mmol, 1 equiv) was added to a round-bottom flask with KI (2 mg, 0.012 mmol, 0.5 equiv) and K_2CO_3 (3 mg, 0.02 mmol, 0.8 equiv). This was dissolved in 1 mL of DMF, followed by addition of the G3 acid (13b) (0.289 g, 0.1 mmol, 3.7 equiv), and the reaction mixture was stirred at room temperature. The reaction was monitored by TLC (3:1 DCM:hexanes). After 5 days, the mixture was diluted in DCM (5 mL), washed with 20% NaHSO_4 (4×10 mL), and dried. The product was separated by column chromatography (3:1 DCM:hexanes, 100% DCM), and



SCHEME 1 Synthesis of G1 to G4 dendrons.

precipitated in hexanes to give 0.201 g of a white powder (53%). SEC: $M_w = 13,350$ g/mol, $M_w/M_n = 1.08$.

^1H NMR (600 MHz, CDCl_3): $\delta = 1.05$ (broad s, 6 H), 1.14 (broad s, 15 H), 1.30–2.3 (broad m), 2.36 (t, $J = 7.0$ Hz, 16 H), 3.20 (t, $J = 7.5$ Hz, 16 H), 4.16–4.26 (broad m, 28 H), 4.89–5.03 (m, 2 H), 6.3–7.5 (broad m), and 7.65–8.15 (m, 72 H). ^{13}C NMR (150 MHz, CDCl_3): $\delta = 14.3$, 17.5, 17.9, 21.1, 22.3, 26.6, 28.4–28.6, 32.6, 33.6, 40.5, 40.8, 41.6–46.7, 53.5, 60.5, 65.2, 65.3, 66.1, 123.2–131.4, 135.5, 145.2–146.2, 171.2, 171.5, 172.1, and 172.9.

Synthesis of PS-G4-Py₁₆ (14c)

11.5 kDa Polystyrene (0.300 g, 0.026 mmol, 1 equiv) was added to a round-bottom flask with KI (2 mg, 0.012 mmol, 0.5 equiv) and K_2CO_3 (3 mg, 0.02 mmol, 0.8 equiv). This was dissolved in 0.5 mL of DMF, followed by addition of the G4 acid (14b) (0.590 g, 0.1 mmol, 3.7 equiv), and the reaction mixture was stirred at room temperature. The reaction was monitored by TLC (3:1 DCM:hexanes). After 7 days, the mixture was diluted in DCM (5 mL), washed with 20% NaHSO_4 (4 \times , 10 mL), and dried. The product was separated by column chromatography (3:1 DCM:hexanes, 100% DCM), and precipitated in hexanes to give 0.178 g of white solid (39%). SEC: $M_w = 14,340$ g/mol, $M_w/M_n = 1.07$.

^1H NMR (600 MHz, CDCl_3): $\delta = 1.11$ (broad s), 1.16 (s), 1.20 (broad s), 1.32–2.17 (broad m), 2.35 (broad triplet, $J = 7.0$ Hz, 32 H), 3.16 (broad triplet, $J = 7.6$ Hz, 32 H), 4.01–4.47 (broad m, 60 H), 4.95–5.05 (m, 2 H), 6.28–7.38 (broad m), and 7.57–8.16 (m, 144 H). ^{13}C NMR (150 MHz, CDCl_3): $\delta = 14.3$, 17.4, 17.6, 17.9, 20.8–22.3, 26.6, 28.4, 28.6, 32.6, 33.6, 40.3–40.8, 43.6–46.8, 60.5, 65.1, 65.6, 123.1–131.4, 135.5, 145.1–146.2, 171.4, 171.5, 171.8, 172.1, and 172.9.

Preparation of Nanotube–Polymer Complexes

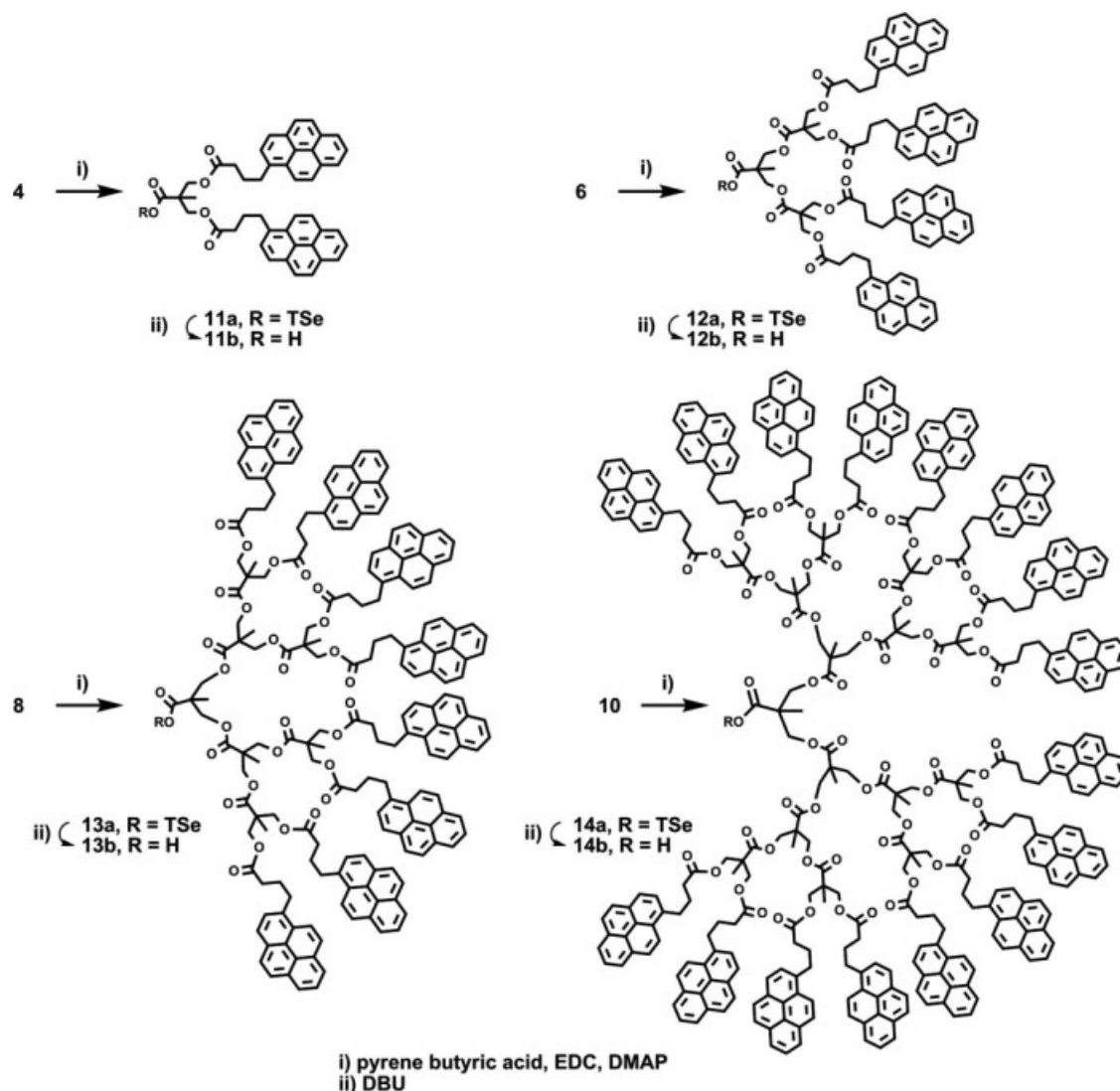
Nanotube solutions were prepared by mixing exactly 2.0 mg of shortened SWNTs (measured on an analytical balance

accurate to five decimal places) with equimolar amounts (5×10^{-4} mmol) of each linear-dendritic polymer (G0 to G4) in 5 mL of THF. The mixtures were ultrasonicated for 10 min and then filtered through a plug of glass wool (in a pipette) until the filtrate was clear and homogeneous. The same procedure was followed for full-length SWNTs and MWNTs, using 2.0 mg of the nanotubes for each experiment. All spectrophotometric measurements were performed in triplicate, and average values are reported.

RESULTS AND DISCUSSION

Preparation of aliphatic polyester dendrons that were peripherally functionalized with pyrene units was accomplished by a divergent synthetic strategy based on the 2,2-bis(hydroxymethyl)-propanoic acid (bis-MPA) building block.^{87,89} The resulting poly(2,2-bis(hydroxymethyl)-propanoic acid) (PMPA) dendrimer structures, initially reported by Ihre et al.,⁹⁰ can be easily and efficiently prepared by nucleophilic attack on the benzylidene protected anhydride of bis-MPA.⁸⁷ The easily removable core protecting group, 2-toluenesulfonyl ethanol (TSe) (**1**) was used to react with anhydride **2** to produce the first generation protected dendron (**3**), as depicted in Scheme 1.⁸⁸ Deprotection using standard hydrogenolysis conditions resulted in the first generation diol **4**. Subsequent iterative reaction with the anhydride **2**, followed by hydrogenolysis, enabled divergent construction of dendrons up to the fourth generation (Scheme 1). It should be noted that the TSe protecting group was stable to all coupling and deprotection reactions, and all products were purified by simple extraction, followed by precipitation (i.e., no column chromatography was required).⁸⁸

Introduction of pyrene groups at the dendron periphery was accomplished by esterification with 4-(1-pyrenyl) butyric acid (PyCOOH), using 1-[3-(dimethylamino)propyl]-3-ethylcarbodiimide (EDC) as the coupling agent (Scheme 2). For



SCHEME 2 Synthesis of pyrene-functionalized dendrons.

generations 1 and 2 (G1, G2), the peripheral functionalization was driven to completion with a small excess of PyCOOH (1.2 equiv per OH), allowing the reaction to proceed overnight. Not surprisingly, the G3 and G4 dendrons required a significantly larger excess of PyCOOH (~ 2 equiv per OH) and, in the case of G4, complete conversion also required a longer reaction time, in excess of 5 days. These coupling reactions could be easily monitored by MALDI-TOF mass spectrometry. For the G4 species, the crude reaction after 48 h showed a distribution of products separated by 272 mass units, attributed to structures having a varying number of PyCOOH groups. After 5 days of stirring, this product distribution coalesced into a single substance having a molecular weight corresponding to the fully pyrene-functionalized G4 dendron. Figure 1 shows the MALDI-TOF MS data for the G2, G3, and G4 dendrons.

Removal of the TSe groups using DBU liberated the desired pyrene-functionalized dendrons having a carboxylic acid group at their core. This approach is advantageous as the

conditions for deprotection of the TSe group are mild, high yielding, and enable easy product purification by extraction into ethyl acetate or dichloromethane followed by precipitation into hexanes.⁸⁸ The removal of the TSe group was confirmed by the disappearance of several diagnostic signals in the ^1H NMR spectrum (Fig. 2). The signals from the para-substituted aromatic ring (7.05 and 7.60 ppm) were no longer visible, providing the clearest evidence for the successful, high-yielding deprotection step. There was also a loss of the signal at 4.31 ppm from the CH_2 protons of the protecting group, but overlap with signals from the dendron backbone along with the butyl esters of the peripheral pyrene linkers limited the diagnostic utility of this signal.

Several options are available when preparing linear-dendritic hybrid polymers.^{91–95} In our case, we chose to prepare the polymer and dendrons separately and then covalently link the two. A sample of polystyrene (PS, $M_w = 11.5$ kDa, PDI = 1.09) was first prepared by nitroxide-mediated radical polymerization (NMP) using the unimolecular nitroxide initiator

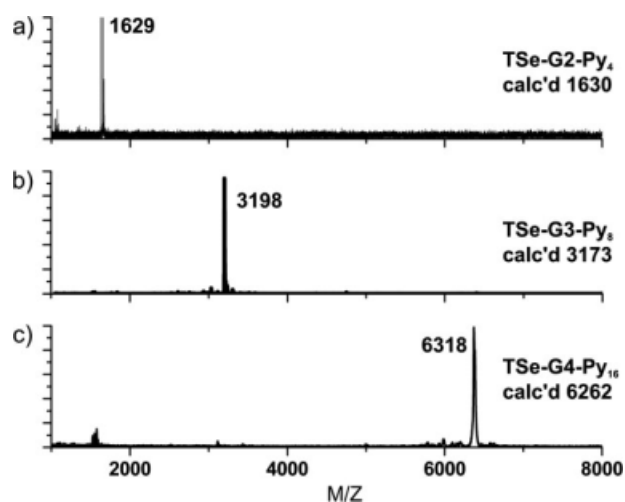


FIGURE 1 MALDI-TOF mass spectral data for (a) TSe-G2-Py₄, (b) TSe-G3-Py₈, and (c) TSe-G4-Py₁₆. Calculated molecular weights are 1630, 3173, and 6262 g/mol, respectively.

developed by Hawker and coworkers.^{96,97} The resulting polystyrene, having a chloromethyl group at one end, could be coupled to the G1 to G4 dendrons having a carboxylic acid group at their core under basic conditions (K₂CO₃, KI), as shown in Scheme 3. Additionally, PyCOOH was coupled to the polymer under the same conditions to produce a G0 control compound. Once again, as the dendron size increased, increasing amounts of excess dendron were required to drive the coupling reaction to completion. Purification of the linear-dendritic hybrids was accomplished by column chromatography to remove the excess dendron and any unreacted polystyrene from the mixture.

Characterization of the linear-dendritic hybrids was accomplished by ¹H NMR and ¹³C NMR, and gel permeation chromatography (GPC). Proton NMR data clearly indicated the presence of signals corresponding to the pyrene-functionalized dendrons, as well as the polystyrene chain. Using a photodiode array detector, GPC provided conclusive evidence that formation of the linear-dendritic hybrids had occurred. The three-dimensional plot depicted in Figure 3 for the PS-G4 hybrid shows that, at the retention time corresponding to the polymer, pyrene absorption from the dendron is clearly observable. Since the retention time of the dendron is signifi-

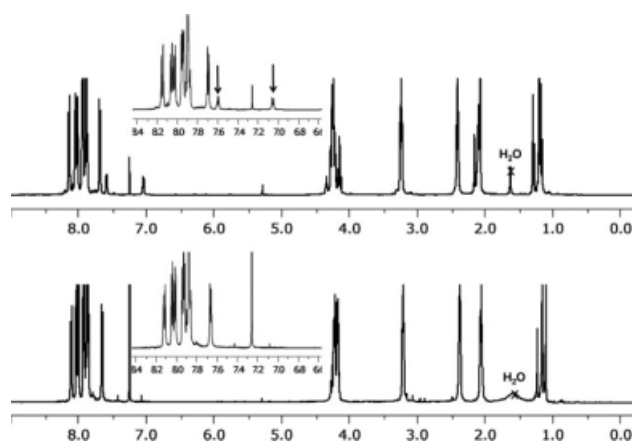
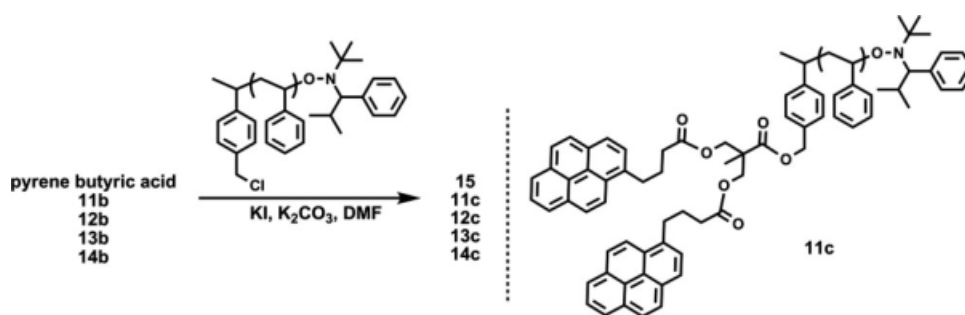


FIGURE 2 ¹H NMR of TSe-G4-Py₁₆ **13a** (top) and COOH-G4-Py₁₆ **13b** (bottom) showing the clean disappearance of signals corresponding to the TSe protecting group (identified with arrows). Insets show close-up views of the spectral region between 6.8 and 8.2 ppm.

cantly different from that of the polymer, this data proves that formation of the linear-dendritic hybrid was successful. It should be noted that the small signal that appears at 22 min in this plot corresponds to a miniscule amount of residual unreacted dendron (much <1%), which proved impossible to remove by column chromatography. Table 1 provides molecular weight data (based on GPC results) for all the linear-dendritic hybrid polymers prepared in this study.

Both the dendrons and the linear-dendritic hybrids were studied by UV-Vis and fluorescence spectroscopy. The spectral data for the linear-dendritic hybrid polymers are depicted in Figure 4. Solutions of these polymers were prepared by dissolving equimolar amounts of each polymer in THF, and the data in Figure 4(A) shows the approximate doubling of pyrene absorption expected with each increase in dendron generation. The steady state fluorescence spectra given in Figure 4(B) were normalized to monomer emission, allowing clear observation of the increase in pyrene excimer emission (centered around 480 nm) with increasing generation. This indicates that the pyrene groups at the dendrimer periphery are relatively mobile, even at the higher generations, and should be capable of orienting themselves around the sidewall of a CNT for optimal π -stacking interactions.



SCHEME 3 Preparation of linear-dendritic hybrid polymers.

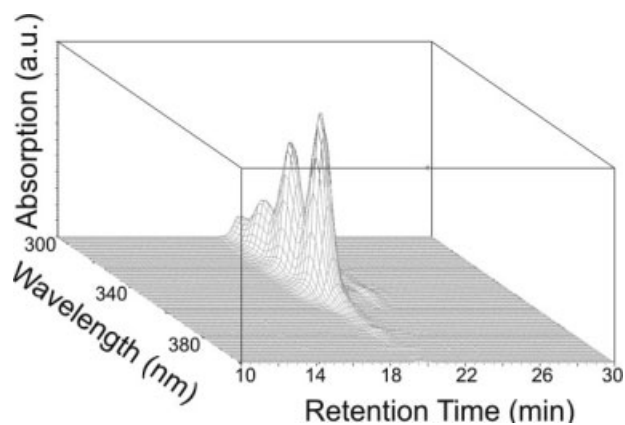


FIGURE 3 Size exclusion chromatography data using a photodiode array UV-Vis detector for the characterization of the PS-G4 linear-dendritic hybrid, showing the characteristic absorption spectrum of pyrene units at the retention time corresponding to the polymer hybrid product.

With the linear-dendritic hybrids in hand, it was possible to investigate their interactions with CNTs in solution. As illustrated in Figure 5, it was expected that the pyrene units of the linear-dendritic hybrid polymers would π -stack to the surface of the SWNTs, effectively anchoring them to the nanotubes. This would result in polystyrene chains extending from the nanotube surface into solution, serving as solubilizing groups for the polymer-nanotube complexes. To maintain consistency with previous work, initial investigations were conducted with shortened SWNTs (having lengths on the order of 350 nm), as they were expected to have greater solubility than as-purchased, full-length SWNTs.^{79,23,36,98} Solutions were prepared by separately mixing equimolar amounts (5×10^{-4} mmol) of each pyrene-labeled linear-dendritic hybrid polymer (G1 to G4, along with the control G0 compound) with a constant mass (2 mg) of the shortened SWNTs in 5 mL of THF. The resulting mixtures were ultrasonicated in a bath sonicator for 10 min, and the solutions were subsequently filtered through a plug of glass wool (in a

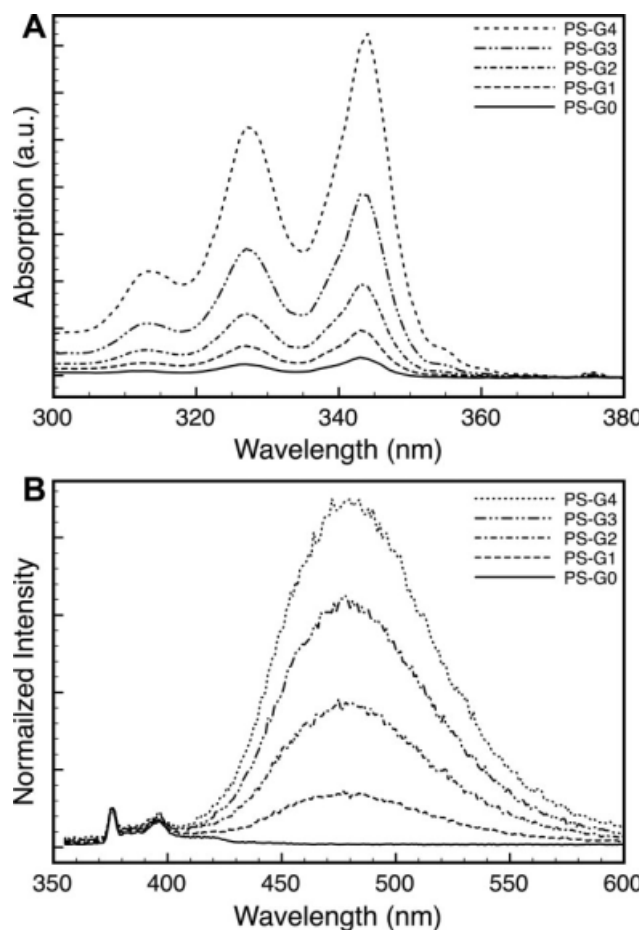


FIGURE 4 (A) UV absorbance and (B) fluorescence spectra of linear-dendritic hybrids in THF. Fluorescence spectra are normalized to monomer emission at 376 nm.

Pasteur pipette) to remove any visible insoluble particulate. The filtered solutions were then investigated to determine nanotube concentration. It should be noted that allowing the solutions to stand for a period of several days did not lead

TABLE 1 Molecular Weights and Polydispersities of Pyrene-Containing Species, Before and After Coupling to the 11.5 kDa Polystyrene

Starting Material	Starting Mol. Wt. (g/mol)	Hybrid Mol. Wt. ^a (g/mol)	PDI ^a
Polystyrene	11,500 ^a	NA	1.09
Pyrene butyric acid	288 ^b	12,000	1.10
11b (G1 acid)	675 ^b	12,300	1.07
12b (G2 acid)	1,630 ^b	13,000	1.06
13b (G3 acid)	3,173 ^b	13,500	1.08
14b (G4 acid)	6,262 ^b	14,300	1.06

^a Determined by GPC.

^b Calculated molecular weight of discrete pyrene-containing species.

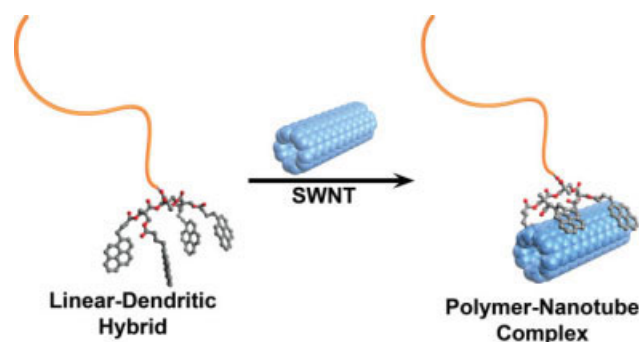


FIGURE 5 Schematic illustration of the interaction between a linear-dendritic hybrid polymer (second generation dendron) and a SWNT (molecular mechanics optimizations of the dendritic segment in both the linear-dendritic hybrid and the polymer-nanotube complex were carried out using the Universal Force Field provided with the software package Avogadro).

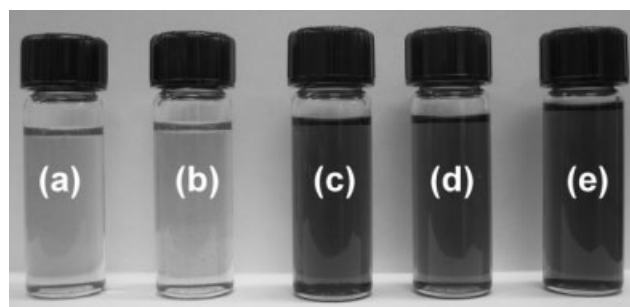


FIGURE 6 Photograph of SWNTs mixed with pyrene-labeled polymer hybrids **15** (a), **11c** (b), **12c** (c), **13c** (d), and **14c** (e) in THF.

to any observable precipitation of solubilized nanotubes. Based on visual inspection, it was clear that nanotube mixtures with polymers coupled to higher generation dendrons exhibited higher nanotube concentrations (see photograph of the solutions, Fig. 6).

Raman spectroscopy, using 785 nm laser excitation, was used to confirm that the observed solutions actually contained SWNTs. Figure 7 compares the Raman spectra of pristine shortened SWNTs, which were simply suspended in THF by sonication, to shortened SWNTs that have been solubilized by the linear-dendritic hybrid **12c** (containing a G2 dendron). In both cases, a drop of the nanotube-containing suspension/solution was deposited on a glass microscope slide and allowed to dry prior to measurement. The spectra in Figure 7 show that the characteristic Raman-active stretching vibrations, including the graphitic G band at $\sim 1590\text{ cm}^{-1}$ and the radial breathing modes (RBM) in the range of $150\text{--}300\text{ cm}^{-1}$, are observable, indicating the presence of SWNTs within the samples. No significant differences are observable between the nanotube samples before and after interaction with the linear-dendritic hybrids, indicating that polymer adsorption does not lead to any structural changes in the nanotube framework. Practically identical

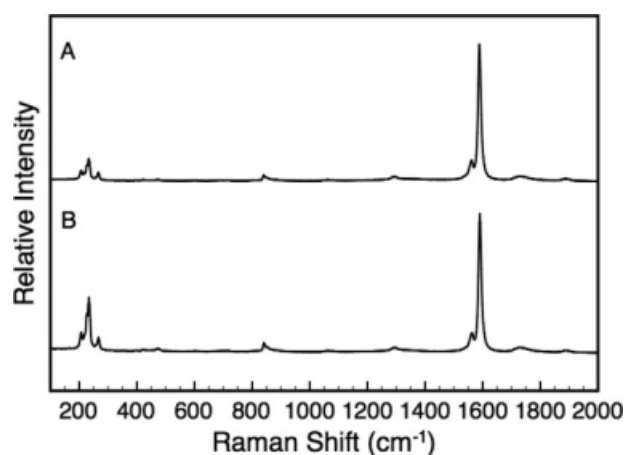


FIGURE 7 Raman spectra (785 nm excitation) of drop-cast samples of pristine shortened SWNTs (A) and shortened SWNTs that were functionalized with the linear-dendritic hybrids (B).

TABLE 2 Linear-Dendritic Polymer Hybrids Mixed with Nanotubes and Resulting Solubilities in THF

Polymer	Number of Pyrenes per Polymer	CNT Concentration (mg/L)
15	1	3 ± 2
11c	2	5 ± 1
12c	4	40 ± 6
13c	8	55 ± 7
14c	16	64 ± 2

results were found with polymers **13c** and **14c** (data not shown).

A more quantitative analysis of nanotube concentration in these mixtures was conducted spectrophotometrically by measuring the absorption of each solution at 500 nm, and using the previously reported specific extinction coefficient for the nanotubes at this wavelength ($\epsilon = 0.0103\text{ L mg}^{-1}\text{ cm}^{-1}$), according to previously published procedures.²³ The measured nanotube concentration values, given in Table 2, show that the concentration of nanotubes in solution exhibits a discontinuous increase when the number of pyrene units per polymer chain increases from 2 to 4. Clearly, the interaction strength between one or two pyrenes with the surface of a CNT is not large enough to overcome the entropic and enthalpic forces associated with polymer dissolution in THF, as well as the van der Waals forces responsible for bundling of the nanotubes. Therefore, the polymer hybrids bearing one or two pyrene units do not impart any appreciable solubility to the nanotubes. However, when pyrene multiplicity at the dendron surface reaches a value of 4 or higher, the pyrene-nanotube interaction is large enough to overcome the tendency for the polymer to dissociate into solution and for the nanotubes to rebundle, thereby immobilizing the polymer chains on the nanotube surface. The anchored polystyrene chains then impart the observed solubility via steric stabilization.⁹⁹ It is interesting to note that, although the observed nanotube concentration continues to increase beyond the second generation, the gain in solubility does not increase proportionately to the increase in pyrene number. This indicates that, for a PS chain having an M_w of 11.5 kDa, introduction of four pyrene units is enough to anchor the chain to the nanotube surface. Increasing the pyrene number beyond four results in diminishing returns, possibly because all the pyrene units cannot simultaneously bind to the nanotube surface, as they are crowded within a small area. Some of the peripheral pyrene units may be back-folded within the dendron structure, and do not come in contact with the nanotube surface. A rudimentary molecular modeling/geometry optimization study using a Universal Force Field (UFF) corroborates this hypothesis,¹⁰⁰ as it indicates that, starting with the third generation, there is not enough space on the nanotube surface for all the pyrene units on a given dendron to simultaneously bind (Fig. 8). Certainly, at the fourth generation, the dendrimer is too large to allow all the pyrene units to come in close proximity to

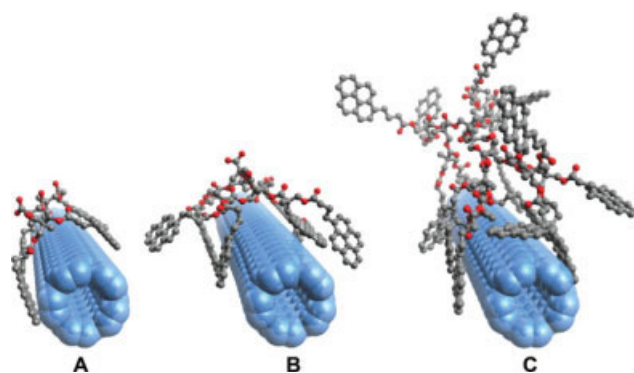


FIGURE 8 Molecular models showing optimized geometries of the G2 (A), G3 (B), and G4 (C) dendrons interacting with the nanotube surface (molecular mechanics optimization was accomplished using the Universal Force Field provided with the Avogadro software package). [Color figure can be viewed in the online issue, which is available at www.interscience.wiley.com.]

the nanotube, and instead extends a number of its chain ends into solution.

The effect of changing polymer molecular weight was also investigated. Two shorter polymers were easily prepared and coupled to the dendrons, while a longer polymer was prepared by chain extending the original 11.5 kDa polystyrene. This longer polymer ($M_w = 18.0$ kDa) was then also coupled to the G2 dendron. We chose to investigate hybrids with the $\text{Py}_4\text{-[G2]-COOH}$ dendron, as this is the smallest structure that imparted appreciable solubility to the nanotubes. The final structures that were investigated included the G2 hybrid polymers where the PS chains had M_w values of 2.5, 4.6, and 18 kDa. Not surprisingly, in the two lower molecular weight cases, the measured nanotube solubility, 7 ± 1 and 29 ± 5 mg/L, respectively, was lower than what was found with the 11.5 kDa polymer. This indicates that, although the interaction of the four pyrene units with the nanotube surface in each of these polymer chains was strong enough to anchor the polymer (based on results described earlier), the shorter PS chains did not serve as strong enough solubilizing groups to match the solubility observed with the 11.5 kDa chains. In the case of the higher molecular weight polystyrene, the nanotube concentrations achieved

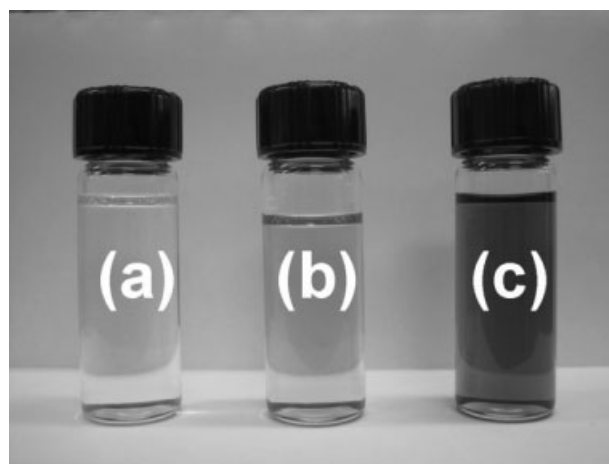


FIGURE 9 Photograph of SWNTs mixed with dendron acids **12b** (a), **13b** (b), and **14b** (c) in THF.

(44 mg/L) were very similar to that of the 11.5 kDa hybrid. This shows that there is no significant difference between using a polymer chain of 11.5 kDa or 18 kDa when trying to stabilize nanotubes in THF with these linear-dendritic hybrids. This result also demonstrates that the G2 dendron is still able to anchor the hybrid structure to the nanotubes even though it is supporting a longer polymer chain.

To determine if the dendrons themselves were capable of imparting any solubility, the dendron acids alone were mixed with SWNTs in THF and treated as described earlier. These experiments were performed with G2 to G4 dendrons, as it was already determined that the G0 and G1 structures do not bind the nanotubes with enough strength to overcome the internanotube van der Waals forces (see earlier). From these experiments, it was found that the G2 and G3 dendrons also did not lead to any significant nanotube solubility [Fig. 9(a,b)]. This was not surprising as these relatively small dendrons are expected to bind to the nanotube surface, but do not exhibit any structural feature that can interact with solvent strongly enough to pull nanotubes into solution. However, the G4 dendron produced a relatively dark solution that, when measured by UV-Vis spectroscopy, exhibited a nanotube concentration of 36 mg/L [Fig. 9(c)]. In this case, the dendron seems to be large enough to simultaneously allow some of the pyrene-functionalized branches to bind to

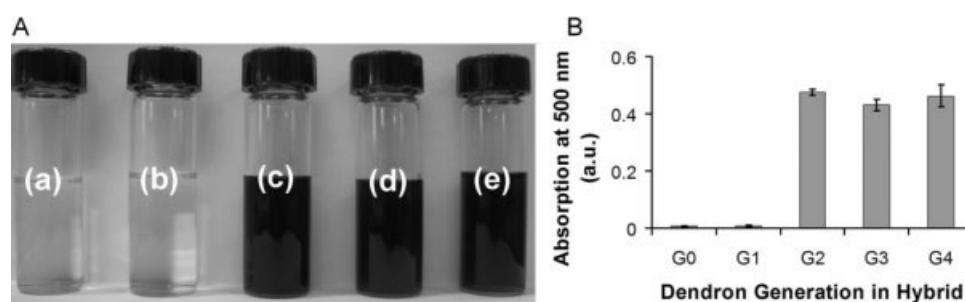


FIGURE 10 (A) Photograph of MWNTs mixed with **15** (a), **11c** (b), **12c** (c), **13c** (d), and **14c** (e) in THF. (B) Plot of MWNT absorption at 500 nm in THF as a function of generation number in the linear-dendritic hybrid polymers.

the nanotube surface while others extend into solution, imparting solubility to the dendron-nanotube complex. This was consistent with what was found in the molecular modeling studies discussed earlier (see Fig. 8).

Considering that the interaction between the pyrene-functionalized linear-dendritic hybrid polymers and shortened SWNTs was strong enough to lead to nanotube solubility, we wished to determine if the same polymers would also impart solubility to full-length nanotubes that were not subjected to any oxidation steps. Using identical procedures to those described earlier (5×10^{-4} mmol of polymer, 2 mg of unshortened SWNTs, and 5 mL of THF), it was found that the SWNTs remained completely insoluble in THF after sonication of the mixture for 10 min, or longer. This is consistent with our previous results using pyrene-functionalized block copolymers, which were also not capable of imparting solubility to full-length SWNTs. The lack of apparent interaction with full-length SWNTs indicates that the binding strength of the polymer to the nanotube surface is not strong enough to overcome the inherent tendency of the full-length nanotubes to bundle together.

With these results in mind, we turned our attention to MWNTs, as several previous reports have described the interaction of both pyrene-containing small molecules and polymers with the surface of MWNTs.^{15,80–83,101–105} Theoretically, the greater diameter of MWNTs results in a decreased surface curvature, which may improve the interaction between the π -system of flat pyrene units and that of the MWNTs. Using the same protocol as described earlier for shortened SWNTs, it was found that the linear-dendritic hybrids of low generation (G0 and G1) had very weak interactions with the full-length MWNTs, whereas the G2 to G4 hybrids were able to stabilize them in solution to a significantly greater extent (Fig. 10). Again, a discontinuous jump in MWNT concentration was observed upon transition from the first to second dendron generation, as clearly indicated in the plot of absorbance values at 500 nm as a function of the dendron generation number [Fig. 10(B)]. This indicates that having four pyrene units per polymer was sufficient to overcome the nanotube bundling interactions and to impart steric stabilization to the MWNTs. Additional pyrene units per polymer did not significantly change MWNT concentrations. Interestingly, when the same MWNTs were mixed with the G4 dendron alone (having no polymer attached) and subjected to the aforementioned treatment, no nanotube solubility was observed. In this case, it is likely that the larger diameter of the MWNTs, relative to SWNTs, allows more pyrene units to bind to the nanotube surface, leaving fewer end-groups to impart solubility. For full-length MWNTs, it therefore appears as though the presence of the polymer solubilizing chain is essential for achieving solubility.

CONCLUSION

From these studies, it is clear that utilizing linear-dendritic polymeric hybrids with peripheral pyrene groups, one can obtain solutions of shortened SWNTs in THF. Increasing the

dendron generation, and therefore number of pyrene units per polymer, gives higher nanotube solubility when mixed with an equal number of polymer chains. A large increase in shortened SWNT solubility was observed on increasing from the first to the second dendron generation, indicating that four pyrene units are necessary to anchor the polymer chains to the nanotube surface and overcome the tendency for nanotubes to form large insoluble bundles. The G4 dendron alone was found to provide stable nanotube solutions, but the lower generation species were not effective. While full-length SWNTs were not dissolved by any of the linear-dendritic hybrids, full-length MWNTs were shown to interact with all of the hybrids in THF, and gave an increasing solubility with increasing dendron generation due to the enhanced interaction between pyrene and a more mildly curved nanotube surface. Here again, a large increase in nanotube solubility was observed on increasing from the second to the third dendron generation, indicating that four pyrene units per polymer are needed to impart significant solubility to MWNTs.

This work was supported by the Natural Science and Engineering Research Council of Canada (NSERC), the Premier's Research Excellence Award (PREA), the Canada Foundation for Innovation (CFI), and the Ontario Innovation Trust (OIT).

REFERENCES AND NOTES

- 1 Tassis, D.; Tagmatarchis, N.; Bianco, A.; Prato, M. *Chem Rev* 2006, 106, 1105–1136.
- 2 Hayashi, T.; Kim, Y. A.; Matoba, T.; Esaka, M.; Nishimura, K.; Tsukada, T.; Endo, M.; Dresselhaus, M. S. *Nano Lett* 2003, 3, 887–889.
- 3 Koerner, H.; Price, G.; Pearce, N. A.; Alexander, M.; Vaia, R. A. *Nat Mater* 2004, 3, 115–120.
- 4 Homenick, C. M.; Lawson, G.; Adronov, A. *Polym Rev* 2007, 47, 265–290.
- 5 Zhao, Y.-L.; Stoddart, J. F. *Acc Chem Res* 2009, 42, 1161–1171.
- 6 Prato, M.; Kostarelos, K.; Bianco, A. *Acc Chem Res* 2008, 41, 60–68.
- 7 Davis, J. J.; Coleman, K. S.; Azamian, B. R.; Bagshaw, C. B.; Green, M. L. H. *Chem Eur J* 2003, 9, 3732–3739.
- 8 Banerjee, S.; Kahn, M. G. C.; Wong, S. S. *Chem Eur J* 2003, 9, 1898–1908.
- 9 Hirsch, A. *Angew Chem Int Ed* 2002, 41, 1853–1859.
- 10 Bahr, J. L.; Tour, J. M. *J Mater Chem* 2002, 12, 1952–1958.
- 11 Sanchez-Pomales, G.; Santiago-Rodriguez, L.; Cabrera Carlos, R. *J Nanosci Nanotechnol* 2009, 9, 2175–2188.
- 12 Sinnott Susan, B. *J Nanosci Nanotechnol* 2002, 2, 113–123.
- 13 Sun, Y.-P.; Fu, K.; Lin, Y.; Huang, W. *Acc Chem Res* 2002, 35, 1096–1104.
- 14 Zhang, Y.; Yuan, S.; Zhou, W.; Xu, J.; Li, Y. *J Nanosci Nanotechnol* 2007, 7, 2366–2375.

- 15** Yang, Q.; Shuai, L.; Pan, X. *Biomacromolecules* 2008, 9, 3422–3426.
- 16** Wu, H.-X.; Tong, R.; Qiu, X.-Q.; Yang, H.-F.; Lin, Y.-H.; Cai, R.-F.; Qian, S.-X. *Carbon* 2007, 45, 152–159.
- 17** Vigolo, B.; Mamane, V.; Valsaque, F.; Le, T. N. H.; Thabit, J.; Ghanbaja, J.; Aranda, L.; Fort, Y.; Mcrae, E. *Carbon* 2009, 47, 411–419.
- 18** Umek, P.; Seo, J. W.; Hernadi, K.; Mrzel, A.; Pechy, P.; Mihailovic, D. D.; Forro, L. *Chem Mater* 2003, 15, 4751–4755.
- 19** Qin, S.; Qin, D.; Ford, W. T.; Resasco, D. E.; Herrera, J. E. *Macromolecules* 2004, 37, 752–757.
- 20** Pastorin, G.; Wu, W.; Wieckowski, S.; Briand, J.-P.; Kostarelos, K.; Prato, M.; Bianco, A. *Chem Commun* 2006, 1182–1184.
- 21** Mcintosh, D.; Khabashesku, V. N.; Barrera, E. V. *J Phys Chem C* 2007, 111, 1592–1600.
- 22** Martinez-Rubi, Y.; Guan, J.; Lin, S.; Scriver, C.; Sturgeon, R. E.; Simard, B. *Chem Commun* 2007, 5146–5148.
- 23** Liu, Y.; Yao, Z.; Adronov, A. *Macromolecules* 2005, 38, 1172–1179.
- 24** Liu, J.; Zubiri, M. R. I.; Dossot, M.; Vigolo, B.; Hauge, R. H.; Fort, Y.; Ehrhardt, J.-J.; Mcrae, E. *Chem Phys Lett* 2006, 430, 93–96.
- 25** Liu, J.; Rodriguez, I.; Zubiri, M.; Vigolo, B.; Dossot, M.; Fort, Y.; Ehrhardt, J.-J.; Mcrae, E. *Carbon* 2007, 45, 885–891.
- 26** Fan, D.-Q.; He, J.-P.; Tang, W.; Xu, J.-T.; Yang, Y.-L. *Eur Polym J* 2006, 43, 26–34.
- 27** D'Souza, F.; Chitta, R.; Sandanayaka, A. S. D.; Subbaiyan, N. K.; D'Souza, L.; Araki, Y.; Ito, O. *J Am Chem Soc* 2007, 129, 15865–15871.
- 28** Dehonor, M.; Masenelli-Varlot, K.; Gonzalez-Montiel, A.; Gauthier, C.; Cavaille, J.-Y.; Terrones, M. *J Nanosci Nanotechnol* 2007, 7, 3450–3457.
- 29** Cheng, F.; Imin, P.; Lazar, S.; Botton, G. A.; de Silveira, G.; Marinov, O.; Deen, J.; Adronov, A. *Macromolecules* 2008, 41, 9869–9874.
- 30** Chang, J.-Y.; Wu, H.-Y.; Hwang, G. L.; Su, T.-Y. *J Mater Chem* 2008, 18, 3972–3976.
- 31** Brunetti, F. G.; Herrero, M. A.; Munoz, J. D. M.; Diaz-Ortiz, A.; Alfonsi, J.; Meneghetti, M.; Prato, M.; Vazquez, E. *J Am Chem Soc* 2008, 130, 8094–8100.
- 32** Gao, C.; He, H.; Zhou, L.; Zheng, X.; Zhang, Y. *Chem Mater* 2009, 21, 360–370.
- 33** Holzinger, M.; Abraham, J.; Whelan, P.; Graupner, R.; Ley, L.; Hennrich, F.; Kappes, M.; Hirsch, A. *J Am Chem Soc* 2003, 125, 8566–8580.
- 34** Holzinger, M.; Vostrowsky, O.; Hirsch, A.; Hennrich, F.; Kappes, M.; Weiss, R.; Jellen, F. *Angew Chem Int Ed* 2001, 40, 4002–4005.
- 35** Bettinger, H. F. *Chem Eur J* 2006, 12, 4372–4379.
- 36** Yao, Z.; Braid, N.; Botton Gianluigi, A.; Adronov, A. *J Am Chem Soc* 2003, 125, 16015–16024.
- 37** Wang, Y.; Iqbal, Z.; Mitra, S. *Carbon* 2005, 43, 1015–1020.
- 38** Tagmatarchis, N.; Prato, M. *J Mater Chem* 2004, 14, 437–439.
- 39** Georgakilas, V.; Tagmatarchis, N.; Pantarotto, D.; Bianco, A.; Briand, J.-P.; Prato, M. *Chem Commun* 2002, 3050–3051.
- 40** Georgakilas, V.; Kordatos, K.; Prato, M.; Guldi, D. M.; Holzinger, M.; Hirsch, A. *J Am Chem Soc* 2002, 124, 760–761.
- 41** Georgakilas, V.; Bourlinos, A.; Gournis, D.; Tsoufis, T.; Trapalis, C.; Mateo-Alonso, A.; Prato, M. *J Am Chem Soc* 2008, 130, 8733–8740.
- 42** Brunetti, F. G.; Herrero, M. A.; de Munoz, J.; Giordani, S.; Diaz-Ortiz, A.; Filippone, S.; Ruaro, G.; Meneghetti, M.; Prato, M.; Vazquez, E. *J Am Chem Soc* 2007, 129, 14580–14581.
- 43** Bayazit, M. K.; Coleman, K. S. *J Am Chem Soc* 2009, 131, 10670–10676.
- 44** Mayo, J. D.; Behal, S.; Adronov, A. *J Polym Sci Part A: Polym Chem* 2009, 47, 450–458.
- 45** Garg, A.; Sinnott, S. B. *Chem Phys Lett* 1998, 295, 273–278.
- 46** Mickelson, E. T.; Huffman, C. B.; Rinzler, A. G.; Smalley, R. E.; Hauge, R. H.; Margrave, J. L. *Chem Phys Lett* 1998, 296, 188–194.
- 47** Piran, M.; Kotlyar, V.; Medina, D. D.; Pirlot, C.; Goldman, D.; Lellouche, J.-P. *J Mater Chem* 2009, 19, 631–638.
- 48** Zhao, Y.; Rice, N. A.; Zhou, N.; Mahmud, I. *ECS Trans* 2008, 13, 31–40.
- 49** Rahman, G. M. A.; Troeger, A.; Sgobba, V.; Guldi, D. M.; Jux, N.; Tchoul, M. N.; Ford, W. T.; Mateo-Alonso, A.; Prato, M. *Chem Eur J* 2008, 14, 8837–8846.
- 50** Nakayama-Ratchford, N.; Bangsaruntip, S.; Sun, X.; Welsher, K.; Dai, H. *J Am Chem Soc* 2007, 129, 2448–2449.
- 51** Cheng, F.; Adronov, A. *Prepr Symp: Am Chem Soc, Div Fuel Chem* 2006, 51, 714–715.
- 52** Zhang, M.; Su, L.; Mao, L. *Carbon* 2005, 44, 276–283.
- 53** Liu, J.; Bibari, O.; Mailley, P.; Dijon, J.; Rouviere, E.; Sauter-Starace, F.; Caillat, P.; Vinet, F.; Marchand, G. *N J Chem* 2009, 33, 1017–1024.
- 54** Chiu, C.-C.; Dieckmann, G. R.; Nielsen, S. O. *Biopolymers* 2009, 92, 156–163.
- 55** Zhang, B.; Xing, Y.; Li, Z.; Zhou, H.; Mu, Q.; Yan, B. *Nano Lett* 2009, 9, 2280–2284.
- 56** Simmons, T. J.; Bult, J.; Hashim, D. P.; Linhardt, R. J.; Ajayan, P. M. *ACS Nano* 2009, 3, 865–870.
- 57** Liu, G.; Wu, B.; Zhang, J.; Wang, X.; Shao, M.; Wang, J. *Inorg Chem* 2009, 48, 2383–2390.
- 58** Backes, C.; Schmidt, C. D.; Hauke, F.; Boettcher, C.; Hirsch, A. *J Am Chem Soc* 2009, 131, 2172–2184.
- 59** Koizhaiganova, R. B.; Kim, H. J.; Vasudevan, T.; Lee, M. S. *Int J Polym Mater* 2009, 58, 120–128.
- 60** Magadur, G.; Lauret, J.-S.; Alain-Rizzo, V.; Voisin, C.; Roussignol, P.; Deleporte, E.; Delaire, J. A. *ChemPhysChem* 2008, 9, 1250–1253.
- 61** Marquis, R.; Greco, C.; Sadokierska, I.; Lebedkin, S.; Kappes, M. M.; Michel, T.; Alvarez, L.; Sauvajol, J.-L.; Meunier, S.; Mioskowski, C. *Nano Lett* 2008, 8, 1830–1835.

- 62** Pascu, S. I.; Kuganathan, N.; Tong, L. H.; Jacobs, R. M. J.; Barnard, P. J.; Chu, B. T.; Huh, Y.; Tobias, G.; Salzmann, C. G.; Sanders, J. K. M.; Green, M. L. H.; Green, J. C. *J Mater Chem* 2008, 18, 2781–2788.
- 63** Ali-Boucetta, H.; Al-Jamal, K. T.; Mccarthy, D.; Prato, M.; Bianco, A.; Kostarelos, K. *Chem Commun* 2008, 459–461.
- 64** Poenitzsch, V. Z.; Winters, D. C.; Xie, H.; Dieckmann, G. R.; Dalton, A. B.; Musselman, I. H. *J Am Chem Soc* 2007, 129, 14724–14732.
- 65** Hughes, M. E.; Brandin, E.; Golovchenko, J. A. *Nano Lett* 2007, 7, 1191–1194.
- 66** Zhao, H.; Yuan, W. Z.; Tang, L.; Sun, J. Z.; Xu, H.; Qin, A.; Mao, Y.; Jin, J. K.; Tang, B. Z. *Macromolecules* 2008, 41, 8566–8574.
- 67** Zhao, H.; Yuan, W. Z.; Mei, J.; Tang, L.; Liu, X. Q.; Yan, M.; Shen, X. Y.; Sun, J. Z.; Qin, A. J.; Tang, Z. *J Polym Sci Part A: Polym Chem* 2009, 47, 4995–5005.
- 68** Zhao, J. J.; Lu, J. P.; Han, J.; Yang, C. K. *Appl Phys Lett* 2003, 82, 3746–3748.
- 69** Tournus, F.; Latil, S.; Heggie, M. I.; Charlier, J. C. *Phys Rev B* 2005, 72, 075431-1–075431-5.
- 70** Paloniemi, H.; Aaritalo, T.; Laiho, T.; Liuke, H.; Kocharova, N.; Haapakka, K.; Terzi, F.; Seeber, R.; Lukkari, J. *J Phys Chem B* 2005, 109, 8634–8642.
- 71** Wu, P.; Chen, X.; Hu, N.; Tam, U. C.; Blixt, O.; Zettl, A.; Bertozzi, C. R. *Angew Chem Int Ed* 2008, 47, 5022–5025.
- 72** Lemek, T.; Mazurkiewicz, J.; Stobinski, L.; Lin, H. M.; Tomasiak, P. *J Nanosci Nanotechnol* 2007, 7, 3081–3088.
- 73** Yang, K.; Wang, X.; Zhu, L.; Xing, B. *Environ Sci Technol* 2006, 40, 5804–5810.
- 74** Chen, R. J.; Zhang, Y.; Wang, D.; Dai, H. J. *J Am Chem Soc* 2001, 123, 3838–3839.
- 75** Ehli, C.; Rahman, G. M. A.; Jux, N.; Balbinot, D.; Guldi, D. M.; Paolucci, F.; Marcaccio, M.; Paolucci, D.; Melle-Franco, M.; Zerbetto, F.; Campidelli, S.; Prato, M. *J Am Chem Soc* 2006, 128, 11222–11231.
- 76** Hoeben, F. J. M.; Jonkheijm, P.; Meijer, E. W.; Schenning, A. *Chem Rev* 2005, 105, 1491–1546.
- 77** Petrov, P.; Stassin, F.; Pagnouille, C.; Jerome, R. *Chem Commun* 2003, 23, 2904–2905.
- 78** Lou, X.; Daussin, R.; Cuenot, S.; Duwez, A. S.; Pagnouille, C.; Detrembleur, C.; Bailly, C.; Jerome, R. *Chem Mater* 2004, 16, 4005–4011.
- 79** Bahun, G. J.; Wang, C.; Adronov, A. *J Polym Sci Part A: Polym Chem* 2006, 44, 1941–1951.
- 80** Choi, I. H.; Park, M.; Lee, S.-S.; Hong, S. C. *Eur Polym J* 2008, 44, 3087–3095.
- 81** Chen, G.; Wright, P. M.; Geng, J.; Mantovani, G.; Haddleton, D. H. *Chem Commun* 2008, 1097–1099.
- 82** Yuan, W. Z.; Mao, Y.; Zhao, H.; Sun, J. Z.; Xu, H. P.; Jin, J. K.; Zheng, Q.; Tang, B. Z. *Macromolecules* 2008, 41, 701–707.
- 83** Xue, C.-H.; Zhou, R.-J.; Shi, M.-M.; Gao, Y.; Wu, G.; Zhang, X.-B.; Chen, H.-Z.; Wang, M. *Nanotechnology* 2008, 19, 215604/215601–215604/215607.
- 84** Meuer, S.; Braun, L.; Zentel, R. *Chem Commun* 2008, 3166–3168.
- 85** Yuan, W. Z.; Sun, J. Z.; Dong, Y.; Haeussler, M.; Yang, F.; Xu, H. P.; Qin, A.; Lam, J. W. Y.; Zheng, Q.; Tang, B. Z. *Macromolecules* 2006, 39, 8011–8020.
- 86** Woo, S.; Lee, Y.; Sunkara, V.; Cheedarala, R. K.; Shin, H. S.; Choi, H. C.; Park, J. W. *Langmuir* 2007, 23, 11373–11376.
- 87** Ihre, H.; Jesus, O. L. P. D.; Frechet, J. M. J. *J Am Chem Soc* 2001, 123, 5908–5917.
- 88** Parrott, M. C.; Benhabbour, S. R.; Saab, C.; Lemon, J. A.; Parker, S.; Valliant, J. F.; Adronov, A. *J Am Chem Soc* 2009, 131, 2906–2916.
- 89** Malkoch, M.; Malmstrom, E.; Hult, A. *Macromolecules* 2002, 35, 8307–8314.
- 90** Ihre, H.; Hult, A.; Soderlind, E. *J Am Chem Soc* 1996, 118, 6388–6395.
- 91** Leolukman, M.; Paoprasert, P.; Mandel, I.; Diaz, S. J.; Mcgee, D. J.; Gopalan, P. *J Polym Sci Part A: Polym Chem* 2009, 47, 5017–5026.
- 92** Vestberg, R.; Piekarski, A. M.; Pressly, E. D.; van Berkel, K. Y.; Malkoch, M.; Gerbac, J.; Ueno, N.; Hawker, C. J. *J Polym Sci Part A: Polym Chem* 2009, 47, 1237–1258.
- 93** Leduc, M. R.; Hawker, C. J.; Dao, J.; Frechet, J. M. J. *J Am Chem Soc* 1996, 118, 11111–11118.
- 94** Gitsov, I. *J Polym Sci Part A: Polym Chem* 2008, 46, 5295–5314.
- 95** Xu, J. T.; Boyer, C.; Bulmus, V.; Davis, T. P. *J Polym Sci Part A: Polym Chem* 2009, 47, 4302–4313.
- 96** Benoit, D.; Chaplinski, V.; Braslau, R.; Hawker, C. J. *J Am Chem Soc* 1999, 121, 3904–3920.
- 97** Hawker, C. J.; Bosman, A. W.; Harth, E. *Chem Rev* 2001, 101, 3661–3688.
- 98** Liu, Y. Q.; Adronov, A. *Macromolecules* 2004, 37, 4755–4760.
- 99** Napper, D. H. *Polymeric Stabilization of Colloidal Dispersions*; Academic Press: London, 1983.
- 100** Avogadro Software Package, Version 0.9.5 released 2009-06-02. Cross-platform open source software available from <http://avogadro.openmolecules.net>.
- 101** Meuer, S.; Braun, L.; Schilling, T.; Zentel, R. *Polymer* 2009, 50, 154–160.
- 102** Gao, Y.; Shi, M.; Zhou, R.; Xue, C.; Wang, M.; Chen, H. *Nanotechnology* 2009, 20, 135705 (9 pp).
- 103** Ehli, C.; Guldi, D. M.; Herranz, M. A.; Martin, N.; Campidelli, S.; Prato, M. *J Mater Chem* 2008, 18, 1498–1503.
- 104** Qu, L. W.; Martin, R. B.; Huang, W. J.; Fu, K. F.; Zweifel, D.; Lin, Y.; Sun, Y. P.; Bunker, C. E.; Harruff, B. A.; Gord, J. R.; Allard, L. F. *J Chem Phys* 2002, 117, 8089–8094.
- 105** Yuan, W. Z.; Lam, J. W. Y.; Shen, X. Y.; Sun, J. Z.; Mahtab, F.; Zheng, Q.; Tang, B. Z. *Macromolecules* 2009, 42, 2523–2531.